Metallofullerenes

DOI: 10.1002/ange.201410012

Regioselective Cage Opening of $La_2@D_2(10611)$-C_{72} with 5,6-Diphenyl-3-(2-pyridyl)-1,2,4-triazine**

Michio Yamada, Yasuhiro Muto, Hiroki Kurihara, Zdenek Slanina, Mitsuaki Suzuki, Yutaka Maeda, Yves Rubin, Marilyn M. Olmstead,* Alan L. Balch,* Shigeru Nagase,* Xing Lu, and Takeshi Akasaka**

Abstract: *The thermal reaction of the endohedral metallofullerene $La_2@D_2(10611)$-C_{72}, which contains two pentalene units at opposite ends of the cage, with 5,6-diphenyl-3-(2-pyridyl)-1,2,4-triazine proceeded selectively to afford only two bisfulleroid isomers. The molecular structure of one isomer was determined using single-crystal X-ray crystallography. The results suggest that the [4+2] cycloaddition was initiated in a highly regioselective manner at the C−C bond connecting two pentagon rings of C_{72}. Subsequent intramolecular electrocyclization followed by cycloreversion resulted in the formation of an open-cage derivative having three seven-membered ring orifices on the cage and a significantly elongated cage geometry. The reduction potentials of the open-cage derivatives were similar to those of $La_2@D_2$-C_{72} whereas the oxidation potentials were shifted more negative than those of $La_2@D_2$-C_{72}. These results point out that further oxidation could occur easily in the derivatives.*

Endohedral metal-atom doping in fullerenes provides hybrid molecules of a new class: endohedral metallofullerenes (EMFs).[1,2] EMFs have received significant attention owing to their unique molecular structures and fascinating electronic and magnetic properties. Because of electron transfer from the encapsulated metal atoms to the fullerene cages, the encaged metal atoms are cationic and fullerene cages are anionic. Accordingly, the electronic structures of EMFs are largely different from those of hollow fullerenes. However, the number of synthesizable EMFs is quite limited because of the difficulty in their preparation. The formation of EMFs has relied on poorly controlled physical processes, such as covaporization of carbon and metal atoms by arc-discharge[3] or collisional ion-implantation[4] methods. Furthermore, these methods are not applicable for every metal element. Accordingly, transplantation of metal ions (or cationic clusters) into anionic carbon cages remains a challenging issue for the preparation of novel endohedral fullerenes, such as iron-encaged EMFs that are unavailable by current methods.[5] The utilization of cage-opening reactions is a promising approach to accomplish the organic synthesis of endohedral fullerenes.[6–9] Komatsu and co-workers applied a three-step cage-opening process with C_{60} to create a 13-membered ring orifice that was large enough to enable the introduction of atoms or small molecules into the cage. The first step involved the reaction of C_{60} with a triazine.[10] The reaction proceeded through an initial [4+2] cycloaddition of the triazine with C_{60} followed by extrusion of a nitrogen molecule. Sequential [4+4] and retro [2+2+2] reactions provided an open cage derivative bearing an eight-membered ring orifice. This achievement motivated us to apply the cage opening reaction to EMFs for the eventual transplantation of metal ions.

Herein, we report the cage-opening reaction of a dimetallic EMF, $La_2@D_2(10611)$-C_{72}, with 5,6-diphenyl-3-(2-pyridyl)-1,2,4-triazine (**1**) (Scheme 1). The chiral dimetallofullerene $La_2@D_2(10611)$-C_{72}, which we will abbreviate as $La_2@D_2$-C_{72}, does not follow the isolated pentagon rule (IPR) and contains two pentalene units at opposite ends of the cage. We chose $La_2@D_2$-C_{72}[11] as the scaffold for the present study, because we expected that its reaction with **1** would proceed at the strained pentalene units in a highly regioselective manner. In fact, the carbon atoms at the pentalene units possess the

---

[*] Prof. Dr. M. Yamada, Dr. M. Suzuki, Prof. Dr. Y. Maeda,
Prof. Dr. T. Akasaka
Department of Chemistry, Tokyo Gakugei University
Koganei, Tokyo 184-8501 (Japan)

Y. Muto, Dr. H. Kurihara, Dr. Z. Slanina, Prof. Dr. T. Akasaka
Life Science Center of Tsukuba Advanced Research Alliance,
University of Tsukuba, Tsukuba, Ibaraki 305-8577 (Japan)
E-mail: akasaka@tara.tsukuba.ac.jp

Prof. Dr. Y. Rubin
Department of Chemistry and Biochemistry
University of California, Los Angeles, CA 90095-1569 (USA)
E-mail: rubin@chem.ucla.edu

Prof. Dr. M. M. Olmstead, Prof. Dr. A. L. Balch
Department of Chemistry
University of California, Davis, CA 95616 (USA)
E-mail: mmolmstead@ucdavis.edu
albalch@ucdavis.edu

Prof. Dr. S. Nagase
Fukui Institute for Fundamental Chemistry
Kyoto University, Kyoto 606-8103 (Japan)
E-mail: nagase@ims.ac.jp

Prof. Dr. X. Lu, Prof. Dr. T. Akasaka
School of Materials Science and Engineering
Huazhong University of Science and Technology
Wuhan 430074 (P.R. China)

Prof. Dr. T. Akasaka
Foundation for Advancement of International Science
Ibaraki 305-0821 (Japan)

[**] Financial support from Research Grants (20108001, "π-Space"), (202455006), (24350019), and (22000009) from the Ministry of Education, Culture, Sports, Science, and Technology of Japan. We also thank the U.S. National Science Foundation (Grants CHE-1305125 for A.L.B. and M.M.O., CHE-1112569 for Y.R.) for support.

Supporting information for this article is available on the WWW under http://dx.doi.org/10.1002/anie.201410012.

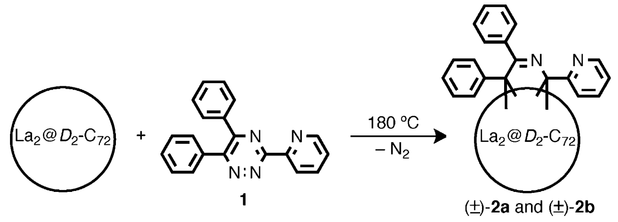

Scheme 1. Reaction of La$_2$@D_2-C$_{72}$ with triazine **1** giving bisfulleroids (±)-**2a** and (±)-**2b**.

highest π-orbital axis vector (POAV)[12] values relative to other carbon atoms in the cage (Supporting Information, Figure S9).

A 1,2-dichlorobenzene solution containing La$_2$@D_2-C$_{72}$ and an excess amount of **1** was heated at 180 °C in a sealed tube for up to 72 h. The reaction solution was analyzed using analytical high-performance liquid chromatography (HPLC). A single new peak was observed under the following conditions: Buckyprep column; eluent, toluene 1 mL min^{-1}. After heating for 72 h, 68 % of La$_2$@D_2-C$_{72}$ was consumed, which was quantitatively converted to the new species. Subsequent HPLC separation using a 5NPE column (eluent, toluene/*n*-hexane/methanol (100:100:1)) successfully afforded two new products (named (±)-**2a** and (±)-**2b**) in a 1:1 ratio (see Figure 1). Matrix-assisted laser desorption ionization-time of flight (MALDI-TOF) mass spectrometry revealed (±)-**2a** and (±)-**2b** to be two bisfulleroid isomers (*m*/*z* 1423.9; Supporting Information, Figure S1). The similarity in their absorption spectra implies that (±)-**2a** and (±)-**2b** have the same addition patterns (Supporting Information, Figure S2). Most absorption features of the parent La$_2$@D_2-C$_{72}$ are retained in the absorption spectra of (±)-**2a** and (±)-**2b**. However, bathochromic shifts result in both cases.

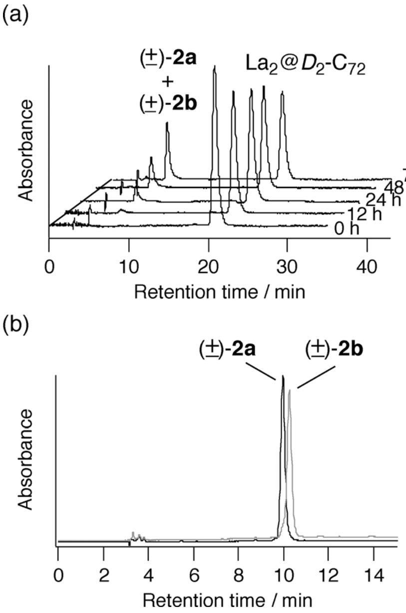

Figure 1. a) HPLC profiles of the reaction mixture. Conditions: Buckyprep column (4.6 mm 250 mm i.d.); eluent, toluene 1 mL min^{-1}. b) HPLC profiles of isolated (±)-**2a** and (±)-**2b**. Conditions: 5NPE column (4.6 mm × 250 mm i.d.); eluent, toluene/*n*-hexane/methanol (100:100:1) 1 mL min^{-1}.

The formation of the bisfulleroid patterns in (±)-**2a** and (±)-**2b** was verified using NMR spectroscopy. The ^{1}H NMR spectrum of (±)-**2a** displays ^{1}H signals corresponding to the two phenyl groups and one pyridyl group (Figure 2). These ^{1}H signals were assigned based on the HSQC and HMBC correlations (Supporting Information, Figures S5 and S6). The ^{13}C NMR spectrum of (±)-**2a** has 88 signals for the sp^2 carbon atoms in the 90–170 ppm region and two signals at 52.6 and 65.7 ppm for the sp^3 carbon atoms (C$_p$ and C$_q$; Supporting Information, Figure S3), suggesting that (±)-**2a** has a C_1 symmetry. Twelve CH signals were identified in the DEPT-135 NMR spectrum of (±)-**2a** (Supporting Information, Figure S4). The bisfulleroid structure of (±)-**2a** was reasonably established from the correlations observed in the HMBC spectrum, in which the correlations between H$_d$–C$_p$, H$_e$–C$_q$, and H$_i$–C$_q$ were clearly observed (Figure 2c; Supporting Information, Figure S6). The NMR spectra also suggest that the rotation of the phenyl ring connecting to the sp^3 carbon atom (C$_q$) was slower than the NMR timescale. Similarly, the respective ^{1}H and ^{13}C NMR spectra of (±)-**2b** indicated the presence of a bisfulleroid structure (Figure 2; Supporting Information, Figures S3–S6). The ^{13}C NMR signals for the sp^3 carbon atoms were observed at 51.7 and 67.1 ppm in (±)-**2b**. Furthermore, 88 carbon signals were found in the 90–170 ppm region, which were ascribable to the sp^2 carbon atoms.

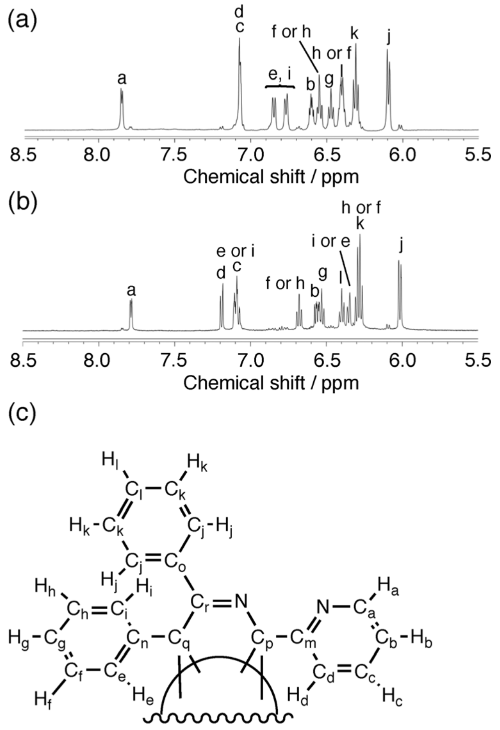

Figure 2. 500 MHz ^{1}H NMR spectra of a) (±)-**2a** and b) (±)-**2b** recorded at 293 K in CS$_2$ ([D$_6$]acetone capillary as lock solvent). c) The NMR numbering of protons (H$_a$–H$_l$) and carbon atoms (C$_a$–C$_r$) of (±)-**2**.

Black crystals of (±)-**2a**·0.5(CS_2) suitable for single-crystal X-ray diffraction (XRD) were obtained by gradual diffusion of *n*-hexane into a solution of (±)-**2a** in CS_2 at 0°C for 3 days.[13] The molecular structure was determined and refined in the space group *C*2/*c* for a data set obtained at 90 K. Based on the crystal structure it is confirmed that the C_{72} portion is derived from the non-IPR cage D_2(10611) possessing two opposing pentalene units.

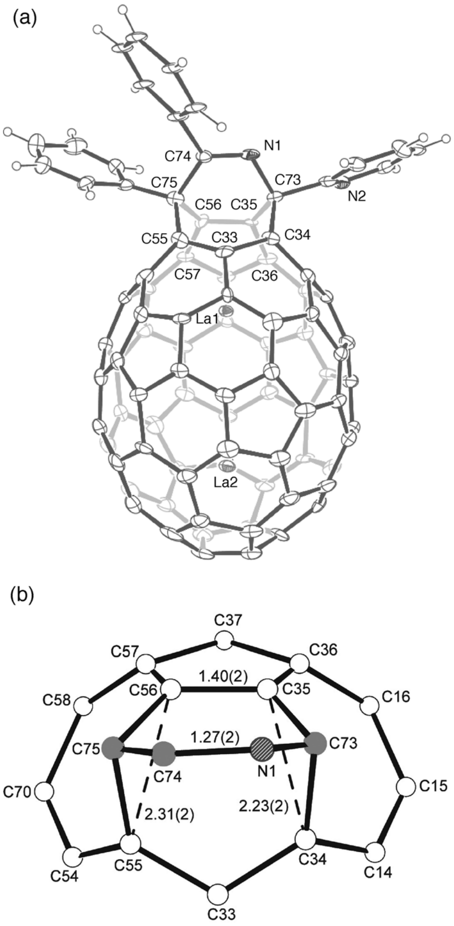

Figure 3. a) A view of the structure of (±)-**2a** at 90 K with ellipsoids set at 30% probability.[13] Solvate molecules are omitted for clarity. b) A top-down view showing the region of adduct formation. Dashed lines show where the bonds have been broken. Atoms C73/C74/C75/N1 are parts of the adduct.

As shown in Figure 3a, addition has occurred only at one end of the D_2(10611)-C_{72} cage. The major La sites (95% for La1 and 93% for La2) are depicted. The La1···La2 distance is 4.357(2) Å. This distance is considerably longer than the La1···La2 distances observed in the structures of three isomers resulting from carbene addition to the $La_2@D_2$-C_{72} cage, namely 4.171, 4.178, and 4.175 Å.[11b] These results confirmed that the initial reaction took place at the central C–C bond of one of the two pentalene units (so-called [5,5] junction), giving three seven-membered ring openings on the cage. These three orifices are shown in the top-down view given in Figure 3b. The dashed lines indicate the connectivity of the non-derivatized cage. Atoms colored in gray are part of the ring-open adduct derived from reaction of $La_2@D_2$-C_{72} and **1**. The bond C35-C56 is the original [5,5] junction and remains intact. Bonds C55–C56 and C34–C35 have been broken and have the new interatomic distances shown. The shortest bond, N1–C74, at 1.27(2) Å, is indicative of its double bond character.

The localization of the high POAV values at the pentalene units appears to dictate the regioselective reaction of $La_2@D_2$-C_{72} with **1**. On the other hand, frontier orbital theory often has difficulty in predicting the kinetically reactive sites of fullerenes, because MOs are, generally speaking, strongly delocalized over the whole spherical surface. In this context, DFT calculations suggest that the HOMO, LUMO + 1, and LUMO + 2 of $La_2@D_2$-C_{72} are delocalized on the carbon cage, whereas the LUMO is located mainly on the internal La atoms (Supporting Information, Figure S10). Based on the fact that the reaction yielded only two regioisomers, it can be deduced that the first reaction step took place exclusively at the [5,5] bond. Because the D_2-C_{72} cage is chiral, the [4+2] addition followed by the N_2 extrusion gives two possible cyclohexadiene intermediates (±)-**3a** and (±)-**3b**. Subsequent electrocyclization reactions followed by cycloreversion generated two regioisomers (isomer A and isomer B), respectively (Figure 4; Supporting Information, Figure S11), though the classification of single- and double-bond character is less clear than that of empty fullerenes. Apparently, (±)-**2a** corresponds to isomer A, as determined by single-crystal XRD. The density functional theory (DFT) calculations suggest that there is a small difference in energy between isomer A and isomer B, and that isomer B is slightly lower in energy (0.255 kcal mol^{-1}) compared to isomer A at the

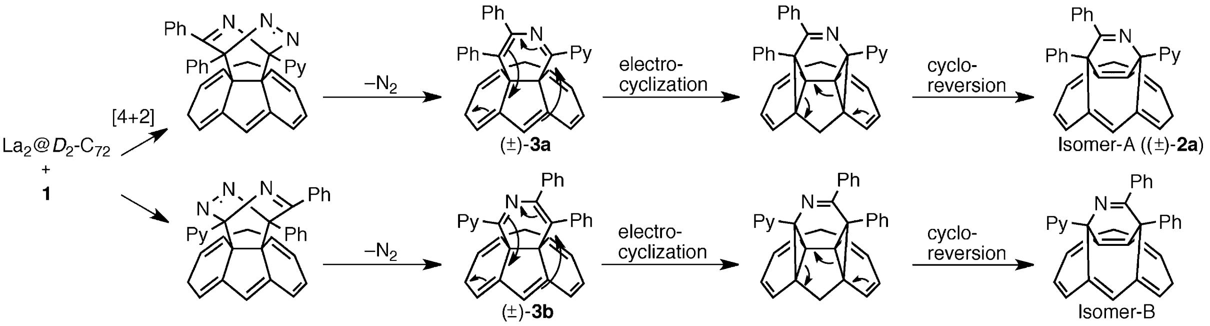

Figure 4. Reaction mechanism for the formation of the two isomers (fullerene partially shown for clarity). Ph = phenyl, Py = 2-pyridyl. The two isomers result from the placement of the addend with the pyridyl group positioned over either the orange or the purple bonds shown in the Supporting Information, Figure S12.

B3LYP/6-31G*~SDD level. In this context, we speculate that (±)-**2b** corresponds to isomer B based on the similarity in the absorption and ^{13}C NMR spectra as well as the electronic properties (see below), though this is not conclusive evidence.

Redox properties are summarized in Table 1. For (±)-**2a** and (±)-**2b**, two single one-electron oxidations and two one-electron reductions were observed, respectively (Supporting Information, Figures S7, S8). The redox potentials of (±)-**2a** and (±)-**2b** are almost identical, implying that they have similar molecular structures. The reduction potentials of (±)-**2a** and (±)-**2b** were similar to those of La$_2$@D_2-C$_{72}$, whereas the oxidation potentials were shifted to more negative values than those of La$_2$@D_2-C$_{72}$. These results point out that further oxidation could occur easily in (±)-**2a** and (±)-**2b**.

Table 1: Redox potentials[a] of (±)-**2a**, (±)-**2b**, La$_2$@D_2-C$_{72}$, and **1**.

Compound	$^2E_{ox}$	$^1E_{ox}$	$^1E_{red}$	$^2E_{red}$
(±)-**2a**	+0.87[b]	+0.12[b]	−0.66	−1.59[b]
(±)-**2b**	+0.88[b]	+0.16[b]	−0.65	−1.58[b]
La$_2$@D_2-C$_{72}$[c]	+0.75[b]	+0.24	−0.68	−0.92
1		+1.82	−1.98	

[a] Values are given in V vs Fc/Fc$^+$ and were obtained using differential pulse voltammetry. [b] Irreversible. [c] Data from Ref. [11b].

In conclusion, we have found that the thermal reaction of La$_2$@D_2-C$_{72}$ with triazine **1** proceeded sequentially to afford two separable bisfulleroid isomers ((±)-**2a** and (±)-**2b**). These results suggest that the initial [4+2] cycloaddition took place selectively at the [5,5] junction bond of the pentalene unit. Further work will be devoted to the oxidation of (±)-**2a** and (±)-**2b** with singlet oxygen, which should result in further enlargement of the orifices.[14]

Received: October 12, 2014
Revised: December 4, 2014

Keywords: cycloadditions · electrochemistry · fullerenes · lanthanum · X-ray diffraction

---

[1] a) *Endofullerenes: A New Family of Carbon Clusters* (Eds.: T. Akasaka, S. Nagase), Kluwer, Dordrecht, **2002**; b) *Chemistry of Nanocarbons* (Eds.: T. Akasaka, F. Wudl, S. Nagase), Wiley, Chichester, **2010**.

[2] a) L. Dunsch, S. Yang, *Small* **2007**, *3*, 1298–1320; b) M. N. Chaur, F. Melin, A. L. Ortiz, L. Echegoyen, *Angew. Chem. Int. Ed.* **2009**, *48*, 7514–7538; *Angew. Chem.* **2009**, *121*, 7650–7675; c) M. Yamada, T. Akasaka, S. Nagase, *Acc. Chem. Res.* **2010**, *43*, 92–102; d) X. Lu, T. Akasaka, S. Nagase, *Chem. Commun.* **2011**, *47*, 5942–5957; e) S. Osuna, M. Swart, M. Solà, *Phys. Chem. Chem. Phys.* **2011**, *13*, 3585–3603; f) A. Rodríguez-Fortea, A. L. Balch, J. M. Poblet, *Chem. Soc. Rev.* **2011**, *40*, 3551–3563; g) X. Lu, L. Feng, T. Akasaka, S. Nagase, *Chem. Soc. Rev.* **2012**, *41*, 7723–7760; h) D. M. Rivera-Nazario, J. R. Pinzón, S. Stevenson, L. Echegoyen, *J. Phys. Org. Chem.* **2012**, *25*, 194–205; i) A. A. Popov, S. Yang, L. Dunsch, *Chem. Rev.* **2013**, *113*, 5989–6113.

[3] Y. Chai, T. Guo, C. Jin, R. E. Haufler, L. P. F. Chibante, J. Fure, L. Wang, J. M. Alford, R. E. Smalley, *J. Phys. Chem.* **1991**, *95*, 7564–7568.

[4] a) R. Tellgmann, N. Krawez, S.-H. Lin, I. V. Hertel, E. E. B. Campbell, *Nature* **1996**, *382*, 407–408; b) E. E. B. Campbell, R. Tellgmann, N. Krawez, I. V. Hertel, *J. Phys. Chem. Solids* **1997**, *58*, 1763–1769; c) A. Gromov, W. Kratschmer, N. Krawez, R. Tellgmann, E. E. B. Campbell, *Chem. Commun.* **1997**, 2003–2004; d) S. Aoyagi et al., *Nat. Chem.* **2010**, *2*, 678–683.

[5] Iron-encaged EMFs can be considered a potential single-molecule device with tunable electronic and magnetic properties.

[6] a) Y. Rubin, *Chem. Eur. J.* **1997**, *3*, 1009–1016; b) Y. Rubin, *Top. Curr. Chem.* **1999**, *199*, 67–91; c) G. Schick, T. Jarrosson, Y. Rubin, *Angew. Chem. Int. Ed.* **1999**, *38*, 2360–2363; *Angew. Chem.* **1999**, *111*, 2508–2512; d) Y. Rubin, T. Jarrosson, G.-W. Wang, M. D. Bartberger, K. N. Houk, G. Schick, M. Saunders, R. J. Cross, *Angew. Chem. Int. Ed.* **2001**, *40*, 1543–1546; *Angew. Chem.* **2001**, *113*, 1591–1594.

[7] a) K. Komatsu, M. Murata, Y. Murata, *Science* **2005**, *307*, 238–240; b) M. Murata, Y. Murata, K. Komatsu, *J. Am. Chem. Soc.* **2006**, *128*, 8024–8033.

[8] K. Kurotobi, Y. Murata, *Science* **2011**, *333*, 613–616.

[9] Y. Morinaka, S. Sato, A. Wakamiya, H. Nikawa, N. Mizorogi, F. Tanabe, M. Murata, K. Komatsu, K. Furukawa, T. Kato, S. Nagase, T. Akasaka, Y. Murata, *Nat. Commun.* **2013**, *4*, 1554.

[10] Y. Murata, M. Murata, K. Komatsu, *Chem. Eur. J.* **2003**, *9*, 1600–1609.

[11] a) H. Kato, A. Taninaka, T. Sugai, H. Shinohara, *J. Am. Chem. Soc.* **2003**, *125*, 7782–7783; b) X. Lu et al., *J. Am. Chem. Soc.* **2008**, *130*, 9129–9136.

[12] R. C. Haddon, *Science* **1993**, *261*, 1545–1550.

[13] CCDC 1010740 ((±)-**2a**) contains the supplementary crystallographic data for this paper. These data can be obtained free of charge from The Cambridge Crystallographic Data Centre via www.ccdc.cam.ac.uk/data_request/cif.

[14] Related oxidation of Sc$_3$N@I_h-C$_{80}$ that form orifices has been reported: G.-W. Wang, T.-X. Liu, M. Jiao, N. Wang, S.-E. Zhu, C. Chen, S. Yang, F. L. Bowles, C. M. Beavers, M. M. Olmstead, B. Q. Mercado, A. L. Balch, *Angew. Chem. Int. Ed.* **2011**, *50*, 4658–4662; *Angew. Chem.* **2011**, *123*, 4754–4758.